Levels of nitramines and nitrosamines in lake drinking water close to a CO_2 capture plant: A modelling perspective

Magnus D. Norling, François Clayer, Cathrine B. Gundersen [*]

Norwegian Institute for Water Research (NIVA), Økernveien 94, 0579 Oslo, Norway

ABSTRACT

While CO_2 capture is considered a key climate change mitigation option, we must ensure that global implementation occurs without causing harm to the local environment and the human health. The most mature option for capture is using amines, which however, is associated with a risk of contaminating nearby drinking water sources with carcinogenic nitramines (NAs) and nitrosamines (NSAs). Here we present the first process-based simulation of NAs and NSAs in a catchment-lake system with the input of previously modelled atmospheric deposition rates. Considering full-scale CO_2 capture at the Oslo waste incineration plant in Norway, future (~10 y) levels in a nearby lake approach the national drinking water limit. We further quantified the effect of hydrological and biogeochemical processes and identified those with the highest sensitivity (NA biodegradation). The uncertainty of the results is presented by a probabilistic distribution (Monte Carlo analysis), incorporating variability in catchment, lake, and literature NA and NSA parameter values. This modelling tool allows for the site-specific assessment of the abovementioned risks related to amine-based CO_2 capture and aspires to contribute to the sound evaluation of costly amine emission reduction measures.

1. Introduction

The urgency of drastically reducing greenhouse gas emissions has never been clearer (IPCC, 2021). Nearly all emission scenarios relay heavily on CO_2 capture to limit warming to 2 °C (Rogelj et al., 2018). Amine-based CO_2 capture is the most mature option (Dutcher et al., 2015; Leung et al., 2014) and has been the choice at the world's first full-scale capture plants (e.g. Boundary Dam) (Stéphenne, 2014). One critical aspect of the technology, that has not been fully addressed, is the risk of forming carcinogenic NA[1]s and NSA[2]s from the amines used for the capture, and how these can impact nearby drinking water sources (Chen et al., 2018; Mazari et al., 2019; Yu et al., 2017).

Through the atmospheric formation pathway, NAs and NSAs will be directly introduced to the nearby environment (Buvik et al., 2021; Nielsen et al., 2012). This occurs as volatile amines inevitably escape the capture plant with the cleaned flue gas (Gouedard et al., 2012). Independent on the type of amine(s) used, degradation processes inside the capture plant will produce small and fugitive amines (Mazari et al., 2015; Tan et al., 2021). Whenever atmospheric oxidants and NOx are present, NAs and NSAs are formed within days (Choi et al., 2021; Nielsen et al., 2012; Pitts et al., 1978). Following deposition on ground, the NAs and NSAs are expected to be transported with local water flow regime (e.g. overland flow, soil-water, rivers, etc.), resulting from their high water solubility ($logK_{ow}$: −1.7 to 1.36) and low soil sorption potential (Gundersen et al., 2017a; Gunnison et al., 2000). Natural drinking water sources (lakes, rivers, and groundwaters) are thus at risk of receiving NAs and NSAs.

In Norway, a drinking water safety limit for the sum of NAs and NSAs has been set at 4 ng L^{-1} (Låg et al., 2011). Similar low drinking water limits exist in other countries for NSAs only (2 and 10 ng L^{-1} in USA/Germany and England/Wales, respectively) (Nawrocki and Andrzejewski, 2011). There is currently no sufficiently sensitive method available to enable monitoring of NAs and NSAs in water at the required low level (Gundersen et al., 2017b; Lindahl et al., 2014). However, advanced instrumentation enables quantification of the amines emitted directly from the stack (Zhu et al., 2013). In Norway, amine-based CO_2 capture operations must comply to amine emission permits set to protect nearby water sources against NAs and NSAs. The permits are estimated

---

with a conservative approach using atmospheric dispersion and deposition modelling (de Koeijer et al., 2013; Karl et al., 2011, 2015), back-calculating from the safety limit in nearby drinking water sources. Shortcomings include the omission of key catchment hydro-biogeochemical processes with implications on NA and NSA water levels (Karl et al., 2014) and possible accumulation with time.

A few studies are available describing the impact of catchment processing. For the NAs, no efficient degradation pathway has been identified and thus the question of accumulation with time is highly relevant (Chen et al., 2018). From the single biodegradation study available, low decay rates were found for a few of the NAs and NSAs tested (half-lives of 28–35 days) while no biodegradation was observed for most of the NAs and NSAs over the course of their essay (Brakstad et al., 2018). On the contrary, efficient degradation of NSAs has been established through photodegradation (10–35 min in summer and to 60–220 min in winter) (Afzal et al., 2016; Plumlee and Reinhard, 2007; Sørensen et al., 2015). Additional complexity is added when considering catchment- and lake-specific processes such as local flow regime, lake stratification, diffusive air-water exchange, or sediment exchange, and how the local climate can impact the magnitude of the above-mentioned processes (e.g. lake ice-cover influences photodegradation).

In the capital city of Norway, Oslo, the construction of an amine-based CO_2 capture plant is underway at the nation's largest waste incineration plant (Fortum Oslo Varme). Once realized, it will be the world's first of its kind, and with the potential for proliferation at hundreds of similar sites across Europe. Atmospheric dispersion and deposition modelling has identified one nearby lake (Lake Elvåga), serving 10% of the Oslo population with drinking water, at risk of receiving NA and NSA at levels approaching the safety limit (Price and Borgnes, 2019). The work considered only simplified assumptions on catchment degradation processes (4.1% steady-state photo-decay of NSAs only). Costly emission reduction measures are considered, such as reheating the flue gas to reach higher altitudes, providing enhanced dispersion and dilution. However, the realistic need for- and potential positive impact of these measures remains to be quantified.

Here we simulate future lake water concentrations of NAs and NSA following 20 years of full-scale CO_2 capture operations at the waste incineration plant in Oslo using a fully integrated catchment-lake hydrological and biogeochemical model. We show that by combining local catchment descriptors, climatic data, and best available literature information on biogeochemical processing, a catchment model provides more realistic estimates of lake NA and NSA concentrations than current conservative approaches. This innovative method is a step towards providing the industry with more realistic emission permits. A model sensitivity analysis identifies the key remaining uncertain processes and helps assess the impact from the two different operational conditions of reheat versus no reheat.

2. Materials & methods

2.1. Case-study site: Lake Elvåga catchment

Lake Elvåga (1.67 km²; Maximum depth of 51.3 m; 59.8772 N, 10.9089 E) is located about 5 km "downwind" of the planned full-scale amine-based CO_2 capture plant (Fortum Oslo Varme; 59.8401 N, 10.8364 E) within a protected boreal forest catchment (17.1 km²; 192–355 m above sea level; annual precipitation: 802 mm; average temperature: 4.3 °C). The lake is subject to strong seasonality including periodic ice cover, temperature stratification, and mixing. Lake Elvåga is relatively pristine, nutrient-poor, and moderately rich in organic matter (e.g., 8 mg L⁻¹ TOC (Isidorova et al., 2016)). For more information on the lake, see Table S1.

Runoff data (1997–2002) was only available from the nearby catchment, Mariholtputten (NVE, 2006). Data of solar radiation, wind speed, air pressure, relative humidity, and cloud cover was obtained from ERA5 reanalysis data (Copernicus Climate Change Service Climate

Data Store). Note that the wind-speed at Lake Elvåga may be significantly lower than depicted in the gridded reanalysis since the lake is situated in a valley with sharp walls of 60–80 m. Precipitation and air temperature were averaged over the catchment based on gridded data obtained from the Norwegian Meteorological Institute (www.met.no).

2.2. The modelling framework

2.2.1. Catchment model

INCA-Contaminant (Nizzetto et al., 2016) is a high-resolution and dynamic catchment model, building on the hydrology model PERSiST (Futter et al., 2014), that was used to simulate NA and NSA transportation to the lake with soil- and groundwater runoff. Various key hydrological processes were considered, such as the evapotranspiration. By increasing the evapotranspiration, water is removed from the catchment resulting in increased levels of NA and NSA in the runoff to the lake. For a complete list of the hydrological processes see Supporting Information. The model was first calibrated, to best predict area-scale runoff from the nearby Mariholtputten catchment (NVE, 2006), giving values of hydrological parameters that are likely to be close to those for Elvåga.

2.2.2. Lake model

EasyLake is a lake model (Norling and Clayer, 2021), simplified and inspired from MyLake (Saloranta and Andersen, 2007), FLake (Kirillin et al., 2011), and GOTM (Burchard et al., 1999), used to simulate levels of NA and NSA in the lake with the shape approximated by a wedge-shaped volume. All NAs and NSAs entering the lake from the catchment and air were assumed to immediately dissolve into the upper water level (epilimnion). Lake stratification, the seasonal formation of distinct separate thermal layers in the water column, was described by: i) a top layer i.e., the epilimnion (top 4–8 m), which is always hydrologically connected to upstream and downstream waters, and ii) a lower section of the lake, i.e., the hypolimnion, which is isolated from the epilimnion when the lake is stratified. Drinking water is sourced from the hypolimnion. Ice cover formation during winter was also simulated since it impacts both photodegradation and water-air diffusive exchange of compounds. For details on computation of lake temperature, stratification, and ice cover, see Supporting Information.

2.3. Nitramine (NA) and nitrosamine (NSA) molecular properties and deposition rates

The NAs and NSAs were treated as two distinct compound groups. Average values for key physiochemical parameters, governing the behavior of the compounds in the catchment, were computed from literature describing the most studied NAs and NSAs associated with CO_2 capture (e.g., di- and monomethylnitramine, monoetanolnitramine, and N-nitrosodimethylamine) as well as a few classified/patented NAs and NSAs. Note that the enthalpy of phase transfer between air and water was not available, and was instead set to vary within a range typical for semi-volatile substances (ΔH: 5–50 kJ mol⁻¹) (Schenker et al., 2005; Shen and Wania, 2005). See Table S2 for NA and NSA parameter values.

NA and NSA atmospheric dry and wet deposition rates as well as atmospheric concentrations were made available by Norsk Energi (Price and Borgnes, 2019). The data represent a waste incineration capacity of 410 000 tons per year, and with 95% CO_2 capture by the reheat operational condition. This provided amine emission at 0.2 ppmv. The simulation was computed using the 2016 weather which provided the highest NA and NSA formation among their three-year simulations (2015–2017). The deposition rates and concentrations, which were of hourly resolution, were aggregated to daily averages and repeated annually for the duration of the simulation. Annual average deposition rates (dry + wet) were 8.241 and 4.139 ng m⁻² day⁻¹ for NAs and NSAs, respectively. There is a strong seasonal variation with higher rates in spring and lower in the autumn and winter. See Table S4 for monthly

aggregated NA and NSA deposition data. Deposition rates without the reheat emission reduction measure were about twice higher than with reheat.

2.4. Key removal processes

The NSAs photodegradation rate in the lake epilimnion ($R_{photo}^{Nitrosamine}$; ng day^{-1}) was adapted from MyLake (Saloranta and Andersen, 2007) as: $R_{photo}^{NSA} = -OC_{NSA} \times QY_{NSA} \times \frac{f_{UV}}{e_{UV}} \times 86400 \times NSA \times Q_{sw} \times (1 - Albedo) \times Attn$, where *NSA* is the total mass of NSAs (ng), OC_{NSA} is the average optical cross-section of NSAs around 340 nm (m^2 mol Nitro^{-1}), QY_{NSA} is the quantum yield (mol NSA mol photon^{-1}), f_{UV} is the fraction of UV radiation in sunlight (unitless), e_{UV} is the energy of a UV photon at 340 nm (J mol photon^{-1}), Q_{sw} is the incoming shortwave radiation at the lake surface (W m^{-2}), *Albedo* is the water or ice albedo (unitless), and *Attn* is the light attenuation coefficient in the water column calculated from Secchi depth (Table S1). The effect of winter ice-cover on photodegradation was considered by shadowing incoming radiation during the relevant time period through the *Albedo*.

The biodegradation rate (R_{bio}; ng day^{-1}) was formulated as follows for both NAs and NSAs in the catchment and lake: $R_{bio} = Compound \times k_{bio} \times \theta^{(T_{water}-20)/10}$, where *Compound* is the mass (ng) of NA and/or NSA, k_{bio} is the biodegradation rate constant at 20 °C (day^{-1}), θ is the Q10 temperature adjustment coefficient (unitless), and T_{water} is the (mean) water temperature (°C). The parameter θ multiplies the biodegradation by 2 for each temperature change of 10 °C, i.e. for a θ value of 2, at 30 °C the biodegradation rate will be 2 times larger than at 20 °C. The NAs and NSAs were split into two groups of fast and slow biodegradation rates, in accordance with the literature (Brakstad et al., 2018), resulting in four modelled classes in total (fast NA, slow NA, fast NSA, and slow NSA). The p_{fast} parameter denotes the proportion of compounds that are fast degrading. Since aerobic and anaerobic biodegradation of the compounds is similar (Brakstad et al., 2018), the k_{bio} for a given NA or NSA class was the same for all catchment and lake compartments.

The diffusive exchanges between the lake surface and the atmosphere are described by Henry's law. It is dependent on the Henry's constant and the gradient in concentrations between surface water and atmosphere. The mass transfer velocity is modelled as for the river surface in INCA-Contaminants. Given that Lake Elvåga is relatively wind-sheltered as mentioned above, we introduced a diffusive exchange multiplier that allows the diffusive exchange between lake and air to be

reduced by a factor of up to 2.

Aqueous loss of NAs and NSAs by sorption to solids was considered to be negligible due to their high water solubility and low soil sorption rates (Gundersen et al., 2017a; Gunnison et al., 2000). In the catchment compartments, partitioning between compounds that are dissolved and bound to soil organic carbon (including dissolved organic carbon) was simulated based on partitioning coefficients computed from the octanol-water partitioning coefficient (Table S2). In the lake, sorption to suspended solids was turned off. See Table S3 for parameter values.

2.5. Sensitivity analysis (Monte Carlo simulation) and selection of parameter values

The parameters to sample in the Monte Carlo simulation (Table 1) were selected for both having a high uncertainty and a significant impact on the lake NA and NSA concentration (sensitivity). For some of the parameters, a likely value, in addition to a range of values (minimum to maximum), were set based on the literature and our own experiences with modelling similar types of catchments. The likely value was used to compute the results presented in Figs. 1 and 2 while the ranges were
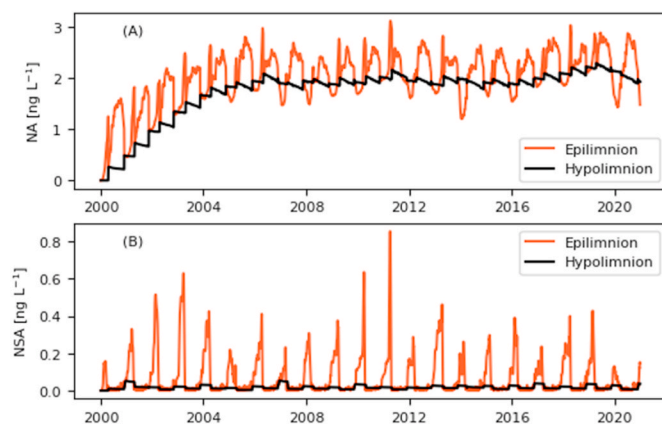

Fig. 1. Modelled time series (2000–2020) of NA (A) and NSA (B) concentrations in the epilimnion/top layer (orange) and in the hypolimnion/bottom layer (black) of the lake, using the "likely" parameter set. (For interpretation of the references to colour in this figure legend, the reader is referred to the Web version of this article.)

Table 1

Key parameters attached to catchment-, lake-, and aqueous removal processes with high uncertainty and sensitivity selected to be sampled in the Monte Carlo simulation. See Supporting Information for parameters not described in the text.

	Parameter name	Unit	Sampling distribution[a]	Likely value	Total effect index
Catchment-Lake Properties	Baseflow index	1	U (0.1, 0.6)	0.2	0.00083
	Degree-day evapotranspiration	mm °C^{-1} day^{-1}	U (0.09, 0.2)	0.14	**0.09433**
	Field capacity	mm	U (30, 150)	50	0.00325
	Groundwater time constant	days	U (50, 150)	75	0.00007
	Soil water time constant	days	U (1, 10)	5.7	0.01155
	Epilimnion winter thickness	m	U (4, 8)	5	0.00076
Aqueous Phase Removal Processes	OC_{NSA} (optical cross-section for photodegradation of NSAs)	m^2 mol^{-1}	U (1.2, 5.0)	2.5	0.00021
	$k_{bio,fast}$ (at 20 °C)	day^{-1}	M(0.02, 0.05, 0.08)	0.05	0.00022
	$k_{bio,slow}$ (at 20 °C)	day^{-1}	M(0.0001, 0.0003, 0.001)	0.0003	**0.43920**
	p_{fast} (proportion of fast-degradable contaminants)	1	M(0.1, 0.2, 0.3)	0.2	**0.14479**
	θ (Q10 temperature response for biodegradation)	1	M(1.2, 2.0, 3.4)	2.0	**0.21452**
	Diffusive exchange multiplier	1	U (0.5, 1)	1	0.02891
	Enthalpy of phase transfer between air and water	kJ mol^{-1}	U (5, 50)	5	**0.09511**
	Fractional size of SOC participating in fast exchange with soil water	1	U (0.1, 0.5)	0.2	0.00002
	Transfer coefficient for exchange between fast and slow SOC fractions	m day^{-1}	U (0.1, 10)	1	0.00003

[a] U signifies a uniform distribution, while M signifies a metalogistic distribution (Keelin, 2016) with the given (5%–50% - 95%) percentiles.
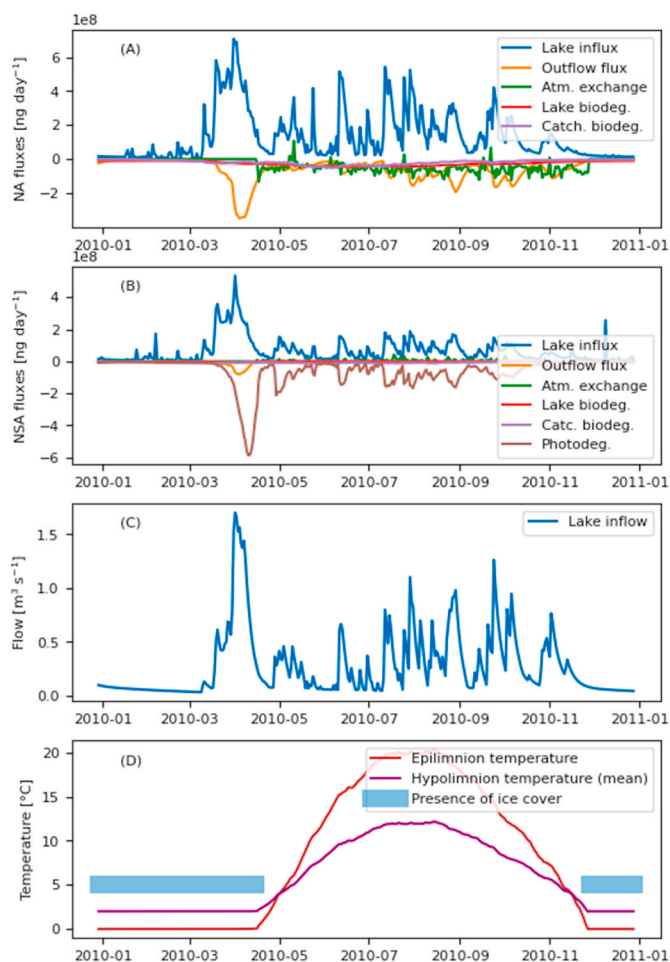
Fig. 2. Modelled time series (2010) of NA (A) and NSA (B) fluxes of lake inflow and direct deposition (blue), lake outflow (orange), lake diffusive exchange with atmosphere (green), lake biodegradation (red), catchment biodegradation (purple), and lake photodegradation (brown, NSA only); (C) lake water inflow (blue); as well as (D) epilimnion (brown) and hypolimnion (purple) lake water temperature and the presence of ice cover (blue), using the "likely" parameter set. Rates are in the in order of 0.1–1 g day^{-1}. (For interpretation of the references to colour in this figure legend, the reader is referred to the Web version of this article.)
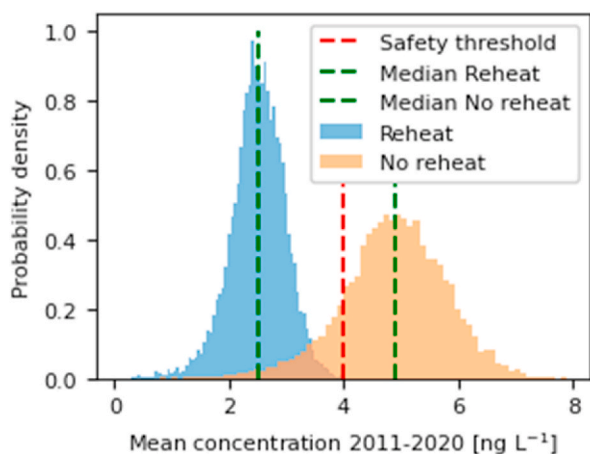

Fig. 3. Distribution of long-term combined average concentrations of NSAs and NAs in the drinking water extracted from the lake, resulting from the Monte Carlo sampling of the parameter space (Table 1).

used to assess the combined effect of parameter uncertainties on the distribution of NA and NSA concentrations (Fig. 3). The Monte Carlo simulation was run once for each of the operational conditions of "reheat" and "no reheat". Since we only had detailed time series data for the reheat scenario, the "no reheat" scenario was set up by multiplying the atmospheric concentration and deposition rates with a factor equal to the ratio between annual averages of the two operational conditions (Price and Borgnes, 2019). A large random sampling (10 000 samples) of the selected parameter space was conducted, while keeping all other parameter values constant (Table S1–3). The Monte Carlo simulation was run from 2000 to 2020 inclusive. The main result statistic was the mean concentration of NAs and NSAs in the hypolimnion (drinking water source) over the last 10 years of the simulation (2011–2020), which we consider representative of long-term concentrations in the water. Here follows a brief discussion on the choice of values for a few of the parameters.

A degree-day evapotranspiration value of 0.14 gave the best fit for predicting runoff evaluated against area scaled Mariholtputten discharge. However, a value of 0.09 was needed to simulate an average 2015–2017 runoff close to the 1961–1990 average runoff of 0.35 m^3 s^{-1} (NVE, 2006). Both these values are within the range included in the Monte Carlo analysis (Table 1). NSA UV-light absorption rates (OC_{NSA}) typically varied within a factor of 2, and was dependent on the specific NSA considered (Plumlee and Reinhard, 2007; Shim et al., 2016). The minimum, likely, and maximum values selected (1.2, 2.5, and 5.0 m^2 mol^{-1}) corresponded to half-lives of 42.8, 85.6, and 178.4 min, respectively. This was in accordance with literature (Afzal et al., 2016; Plumlee and Reinhard, 2007; Sørensen et al., 2015). Biodegradation rates (k_{bio}) for relevant NAs were only found reported by one study (Brakstad et al., 2018) from which the range of possible values for each sub-class of fast- and slow degrading compounds were averaged.

To identify the most influential parameters to the results from the Monte Carlo simulation, the total effect index $S_{T,i}$ of each parameter i was calculated as follows: $S_{T,i} = \frac{E_{X_{\sim i}}(Var_{X_i}(Y|X_{\sim i}))}{Var(Y)}$, where Y is the model output (in this case the mean combined concentration of NAs and NSAs in the lake water extracted during the last 10 years of the simulation), E and Var are the expectation and variance operators respectively, X_i is parameter i, and $X_{\sim i}$ is the set of parameters excluding parameter i. We use a numerical approximation (Saltelli et al., 2010) to compute the indexes. It measures how much of the total variance of the result (over the given parameter space) that can be attributed to each of the parameters. We highlight the indexes that are higher than 0.05. Note that due to interactions between parameters, the indexes can sum to a value that is higher than one.

The lack of measured NSA and NA concentrations rules out many methods for model uncertainty analysis that could otherwise have narrowed down the likely ranges of the parameters.

3. Results and discussion

3.1. Modelled hydrological and lake physical processes

Overall, the representation of hydrology and lake physical processes in our model appear realistic. In brief, the simulated catchment average flow at 0.28 m^3 s^{-1} (Fig. 2C) was only slightly lower than previously estimated runoff maps (0.35 m^3 s^{-1}) (Naserzadeh and Svegården, 2006), likely resulting from the unusual low precipitation in 2016. Expected seasonality was observed in the lake inflow, with the highest flows occurring during autumn events, in accordance with similar catchments in this region (Vormoor et al., 2015). Strong seasonal patterns were also evident in the simulated lake temperature, ranging from 0 to 25 °C (Fig. 2D), agreeing with both previous observations from the lake (Isidorova et al., 2016) and similar lakes in Eastern Norway (Clayer et al., 2021; Couture et al., 2018). Two lake water mixing events were predicted to occur each spring and autumn, with a duration of 1–22 days,

similar to another well-studied Norwegian lake (Clayer et al., 2021). Ice cover lasts from late November/early December to late February/early March with an average duration of 98 days (52–147 days; Fig. 2D), consistent with local observations from small lakes in the region (Solvang, 2013).

3.2. Assessing NA and NSA lake water concentrations in relation to the drinking water safety limit

Constant CO_2 capture using reheat at the Oslo waste incineration plant for the duration of 20 years produced NA and NSA levels in Lake Elvåga below- but close to the safety drinking water limit (Fig. 1A and B and 2). Interestingly, levels of NAs increased with time for approximately seven years before stabilizing at 2.5 ± 0.5 ng L^{-1} and at 2.6 ± 0.5 ng L^{-1} in the hypolimnion and epilimnion, respectively (Fig. 1A). NSA levels were lower, but with strong seasonal epilimnion peaks during winter, reaching 0.8 ng L^{-1}. This indicated different response to key catchment- and lake processes between the two compound groups. NSA and NA lake water levels were lower than the estimates obtained using the atmospheric dispersion and deposition model (3.4 ng L^{-1}) that included steady-state photo-decay of NSAs, but without biodegradation and the possibility of accumulation with time (Price and Borgnes, 2019).

The presented assessment does not consider the possibility of natural background levels of NAs and NSAs adding to the estimates. In the absence of a sufficiently sensitive analytical method the occurrence of these compounds in natural waters cannot be explored. However, their precursor molecule, the amine, is a natural component of environmental systems (Poste et al., 2014) and can also be emitted from other types of anthropogenic activities (Ge et al., 2011). While amines dissolved in natural waters cannot form NAs and NSAs through the atmospheric pathway, alternative NA and NSA formation pathways have been identified in other settings (Kemper et al., 2009; Walse and Mitch, 2008) and cannot be ruled out in natural water systems.

3.3. Governing processes for NA and NSA fluxes in the catchment and the impact from seasonality

The input fluxes to the lake were lower for the NAs than the NSAs (Fig. 2A and B), which contrasted to their lake concentrations. This mainly resulted from photodegradation of the NSAs during the ice-free season, efficiently reducing levels of NSAs towards zero. For the NAs, biodegradation in addition to diffusive exchange with the atmosphere were the most important losses but were insufficient at balancing the input rate. On average, photodegradation removes 82.5% of the incoming NSAs, while biodegradation (in-lake, soil, and groundwater) amounts to 11.3%. For NAs, biodegradation in the soil, groundwater, and lake removes 10.3, 1.2 and 15.2% of the incoming NAs respectively, and air-water diffusive exchange 23.8%.

The peaks in NA concentration were associated with increased inputs to the lake during spring snow melt and to a lesser extent during autumn intense precipitation. For the NSAs, the corresponding higher spring input was mitigated by high rates of photodegradation. The peaking NSAs epilimnion levels are consistently simulated during winter (Fig. 1B), which coincides with the timing of an ice cover (Fig. 2D) that efficiently shields the NSAs from the weaker sunlight radiation occurring during wintertime. This specific seasonal pattern places the snow melt season at higher risk of experiencing combined high NA and NSA concentrations. On the other hand, the highest NA concentrations in the lake epilimnion are found in late summer/early autumn as a result of summer accumulation and weaker removal processes compared to NSAs, just before mixing with the hypolimnion dilutes NAs again.

As pointed out above, biodegradation is the main removal process for NAs and its parameters are loosely constrained due to the lack of knowledge on specific compounds biodegradability. Here our groups of NAs and NSAs have been dictated by the atmospheric dispersion modelling outputs, although biodegradability is compound specific (Brakstad et al., 2018). In fact, the –OH molecular group is believed to be more susceptible to biodegradation than the nitroso- and nitro-substituents (Brakstad et al., 2018). Hence, implementing a compound-specific biodegradation rate in the model would likely reduce uncertainty around the estimated NA concentrations. Thus, additional studies of biodegradation rates under a variety of environmental conditions to represent soil, ground- and lake water as well as to assess the impact of bacterial communities and temperature are further required.

3.4. Lake stratification causes delay in NAs levels

In the lake, the seasonal thermal stratification appears to play an important role for the lake water levels of NA and NSAs. In the epilimnion, the concentrations show clear long-term, seasonal and shorter-term variations while in the hypolimnion the variations are most pronounced during mixing events (Fig. 1A and B). This disparity highlights the relative isolation of the hypolimnion compared to the epilimnion. Seasonal and shorter-term variations are also evident in the various fluxes and process rates of NA and NSA, highlighting the response of these fluxes to, inter alia, hydrological and lake physical forcing.

The impact of lake physical processes, snow melt on contaminant transport and distribution in the catchment has been previously acknowledged (Dueri et al., 2009; Meyer and Wania, 2008) and show strong seasonal variations (Williams et al., 2003). At first, the hypolimnion will act as a buffer for contaminants, diluting and storing the contaminants following mixing with the relatively more contaminated epilimnion. Based on our modelling, seven years are needed for the NA concentration in the hypolimnion reach a semi-steady state (Fig. 1A), in equilibrium with inputs and the various removal fluxes (Fig. 2A). On the long term, this accumulation of contaminant in the hypolimnion can cause further risks for the biota and water consumption. In addition, if NAs deposition within the Elvåga catchment is reduced or stopped, the lake will likely need a similar amount of time to recover.

3.5. Implications of the parameter ranges (Monte Carlo) and the CO_2 capture operational condition ("reheat") against the drinking water limit

Using the range of values set for the most uncertain and influential parameters (Table 1) the Monte Carlo sampling gives a distribution of possible long-term average concentrations in the drinking water extracted from the lake (Fig. 3). This illustrates the probability for a parameter set to result in long-term concentration of NAs and NSAs exceeding the drinking water limit (4 ng L^{-1}) (Låg et al., 2011). By using the "reheat" operational setting, only 0.02% of the sampled parameter sets result in long-term concentrations exceeding the safety limit. Using the higher deposition rates of "no reheat" emission scenario, 85.03% of the sampled parameter sets result in long-term concentrations exceeding the limit. This demonstrates the effectiveness of this measure, providing enhanced dispersion and dilution of the emitted compounds. It should be noted that the sensitivity analysis is only carried out on the catchment-lake model. A more thorough approach would be to do a combined sensitivity assessment on the atmospheric- and catchment-lake models together.

The sensitivity analysis shows that uncertainty in biodegradation by far accounts for most of the uncertainty in the model output (Table 1), followed by evapotranspiration and parameters related to diffusive exchange between the lake and the atmosphere. Thus, the most efficient way to reduce model uncertainty is to get a better understanding of the NA biodegradation rates and related parameters, as described above. Better constraints on catchment hydrology, especially evapotranspiration, would also help reduce uncertainty through e.g., the availability of measured discharge time series for the inlet(s) to the lake. Another path to reducing uncertainty would be to improve analytical method detection limit in order to observe NAs and NSAs in the environment and construct a validation dataset. Furthermore, data on the plant uptake

rate of the nitrogen-rich NAs and NSAs, currently ignored but shown to be significant (Panz and Miksch, 2014), would help further improve the model.

While the present modelling approach is perfectible in many ways, it provides more realistic lake NA and NSA concentrations unlike previous approaches. Importantly, while our modelling approach require local adaptations, it is transferrable to other locations with different types of sensitive water sources, e.g. groundwater, and our model has the potential to couple directly to the output of different types of atmospheric dispersion and deposition models.

Finally, this work aspires to improve the cost efficiency of amine-based CO_2 capture through the presentation of a modelling tool able to quantify realistic NA and NSA levels in natural waters. Our tool can be used to assess the effect of costly amine emission measures and help establishing sound amine emission permits. This work further contributes to the environmental and health risk assessment of amine-based CO_2 capture by predicting future NA and NSA levels in natural waters and identifying key influential and uncertain governing processes. We recommend, as also pointed out earlier (Chen et al., 2018), future work to establish biodegradation rates of the NAs under relevant environmental conditions in order to improve risk and life-cycle assessments of amine-based CO_2 capture. We also recommend the catchment-lake model to be run in conjunction with the atmospheric dispersion and deposition model to enable an overall sensitivity analysis.

Declaration of competing interest

The authors declare the following financial interests/personal relationships which may be considered as potential competing interests: Cathrine Brecke Gundersen reports financial support was provided by COWI Norway AS.

Acknowledgments

Appendix A. Supplementary data

Supplementary data to this article can be found online at https://doi.org/10.1016/j.envres.2022.113581.

References

Afzal, A., et al., 2016. Degradation and fate of N-nitrosamines in water by UV photolysis. Int. J. Greenh. Gas Control 52, 44–51.

Brakstad, O., et al., 2018. Biotransformation in water and soil of nitrosamines and nitramines potentially generated from amine-based CO2 capture technology. Int. J. Greenh. Gas Control 70.

Burchard, H., et al., 1999. GOTM, a General Ocean Turbulence Model. Theory, Implementation and Test Cases.

Buvik, V., et al., 2021. A review of degradation and emissions in post-combustion CO2 capture pilot plants. Int. J. Greenh. Gas Control 106, 103246.

Chen, X., et al., 2018. Emerging N-nitrosamines and N-nitramines from amine-based post-combustion CO2 capture – a review. Chem. Eng. J. 335, 921–935.

Choi, N.R., et al., 2021. Particulate nitrosamines and nitramines in seoul and their major sources: primary emission versus secondary formation. Environ. Sci. Technol. 55, 7841–7849.

Clayer, F., et al., 2021. Boreal headwater catchment as hot spot of carbon processing from headwater to fjord. J. Geophys. Res. Biogeosci. 126, e2021JG006359.

Copernicus Climate Change Service Climate Data Store, Fifth Generation of ECMWF Atmospheric Reanalyses of the Global Climate.

Couture, R.-M., et al., 2018. Simulating water quality and ecological status of Lake Vansjø, Norway, under land-use and climate change by linking process-oriented models with a Bayesian network. Sci. Total Environ. 621, 713–724.

de Koeijer, G., et al., 2013. Health risk analysis for emissions to air from CO2 Technology Centre Mongstad. Int. J. Greenh. Gas Control 18, 200–207.

Dueri, S., et al., 2009. Modelling the influence of thermal stratification and complete mixing on the distribution and fluxes of polychlorinated biphenyls in the water column of Ispra Bay (Lake Maggiore). Chemosphere 75, 1266–1272.

Dutcher, B., et al., 2015. Amine-based CO2 capture technology development from the beginning of 2013—a review. Renew. Sustain. Energy Rev. 7, 2137–2148.

Futter, M., et al., 2014. PERSiST: a flexible rainfall-runoff modelling toolkit for use with the INCA family of models. Hydrol. Earth Syst. Sci. 18, 855–873.

Ge, X., et al., 2011. Atmospheric amines – Part I. A review. Atmos. Environ. 45, 524–546.

Gouedard, C., et al., 2012. Amine degradation in CO2 capture. I. A review. Int. J. Greenh. Gas Control 10, 244–270.

Gundersen, C.B., et al., 2017a. Soil sorption of two nitramines derived from amine-based CO2 capture. Environ. Sci. Process. Impacts. 19, 812–821.

Gundersen, C.B., et al., 2017b. LC–MS/MS method for simultaneous determination of monoethanol- and dimethylnitramine in aqueous soil extracts. Chromatographia 80, 1475–1481.

Gunnison, D., et al., 2000. Attenuation mechanisms of N-nitrosodimethylamine at an operating intercept and treat groundwater remediation system. J. Hazard Mater. 73, 179–197.

IPCC, 2021. Summary for policymakers. In: Masson-Delmotte, V., et al. (Eds.), Climate Change 2021: the Physical Science Basis. Contribution of Working Group I to the Sixth Assessment Report of the Intergovernmental Panel on Climate Change. Cambridge University Press (in press).

Isidorova, A., et al., 2016. The effect of lake browning and respiration mode on the burial and fate of carbon and mercury in the sediment of two boreal lakes. J. Geophys. Res. Biogeosci. . 121, 233–245.

Karl, M., et al., 2014. Uncertainties in assessing the environmental impact of amine emissions from a CO2 capture plant. Atmos. Chem. Phys. 14, 8533–8557.

Karl, M., et al., 2015. Modelling atmospheric oxidation of 2-aminoethanol (MEA) emitted from post-combustion capture using WRF–Chem. Sci. Total Environ. 527–528, 185–202.

Karl, M., et al., 2011. Worst case scenario study to assess the environmental impact of amine emissions from a CO2 capture plant. Int. J. Greenh. Gas Control 5, 439–447.

Keelin, T.W., 2016. The metalog distributions. Decis. Anal. 13, 243–277.

Kemper, J.M., et al., 2009. Nitrosamine, dimethylnitramine, and chloropicrin formation during strong base anion-exchange treatment. Environ. Sci. Technol. 43, 466–472.

Kirillin, G., et al., 2011. FLake-Global: online lake model with worldwide coverage. Environ. Model. Software 26, 683–684.

Leung, D.Y.C., et al., 2014. An overview of current status of carbon dioxide capture and storage technologies. Renew. Sustain. Energy Rev. 39, 426–443.

Lindahl, S., et al., 2014. A review of available analytical technologies for qualitative and quantitative determination of nitramines. Environ. Sci. Process. Impacts. 16, 1825–1840.

Låg, M., et al., 2011. Health Effects of Amines and Derivates Associated with CO2 Capture. The Norwegian Institute of Public Health (NIPH), Oslo, Norway.

Mazari, S.A., et al., 2019. Formation and elimination of nitrosamines and nitramines in freshwaters involved in post-combustion carbon capture process. J. Environ. Chem. Eng. 7, 103111.

Mazari, S.A., et al., 2015. An overview of solvent management and emissions of amine-based CO2 capture technology. Int. J. Greenh. Gas Control 34, 129–140.

Meyer, T., Wania, F., 2008. Organic contaminant amplification during snowmelt. Water Res. 42, 1847–1865.

Naserzadeh, A.R., Svegården, J., 2006. Flomsonekart. Delprosjekt Fjellhamar. The Norwegian Water Resources and Energy Directorate (NVE).

Nawrocki, J., Andrzejewski, P., 2011. Nitrosamines and water. J. Hazard Mater. 189, 1–18.

Nielsen, C.J., et al., 2012. Atmospheric chemistry and environmental impact of the use of amines in carbon capture and storage (CCS). Chem. Soc. Rev. 41, 6684–6704.

Nizzetto, L., et al., 2016. Assessment of contaminant fate in catchments using a novel integrated hydrobiogeochemical-multimedia fate model. Sci. Total Environ. 544, 553–563.

Norling, M.D., Clayer, F., 2021. Mobius Modules: EasyLake, GitHub Repository.

NVE, 2006. In: Naserzadeh, A.R., Svegården, J. (Eds.), Flomsonekart, Delprosjekt Fjellhamar, vol. 5. Norges vassdrags- og energidirektorat (NVE).

Panz, K., Miksch, K., 2014. Phytoremediation of soil contaminated with explosive compounds. In: Singh, S.N. (Ed.), Biological Remediation of Explosive Residues. Springer International Publishing, Cham, pp. 235–257.

Pitts, J.N., et al., 1978. Photooxidation of aliphatic amines under simulated atmospheric conditions: formation of nitrosamines, nitramines, amides, and photochemical oxidant. Environ. Sci. Technol. 12, 946–953.

Plumlee, M.H., Reinhard, M., 2007. Photochemical attenuation of N-nitrosodimethylamine (NDMA) and other nitrosamines in surface water. Environ. Sci. Technol. 41, 6170–6176.

Poste, A.E., et al., 2014. Amines and amine-related compounds in surface waters: a review of sources, concentrations and aquatic toxicity. Sci. Total Environ. 481, 274–279.

Price, C., Borgnes, D., 2019. Dispersion and Deposition Modelling NO2, Nitrosamines and Nitramines. Klemetsrud Carbon Capture Plant. Norsk Energi.

Rogelj, J., et al., 2018. Mitigation pathways compatible with 1.5°C in the context of sustainable development. In: Masson-Delmotte, V., et al. (Eds.), Global Warming of 1.5°C. An IPCC Special Report on the Impacts of Global Warming of 1.5°C above Pre-industrial Levels and Related Global Greenhouse Gas Emission Pathways, in the Context of Strengthening the Global Response to the Threat of Climate Change, Sustainable Development, and Efforts to Eradicate Poverty (in press).

Saloranta, T.M., Andersen, T., 2007. MyLake—a multi-year lake simulation model code suitable for uncertainty and sensitivity analysis simulations. Ecol. Model. 207, 45–60.

Saltelli, A., et al., 2010. Variance based sensitivity analysis of model output. Design and estimator for the total sensitivity index. Comput. Phys. Commun. 181, 259–270.

Schenker, U., et al., 2005. Improving data quality for environmental fate models: a least-squares adjustment procedure for harmonizing physicochemical properties of organic compounds. Environ. Sci. Technol. 39, 8434–8441.

Shen, L., Wania, F., 2005. Compilation, evaluation, and selection of Physical−Chemical property data for organochlorine pesticides. J. Chem. Eng. Data 50, 742–768.

Shim, J.-G., et al., 2016. Effect of pH on UV photodegradation of N-nitrosamines in water. J. Kor. Soc. Water Environ. 32, 357–366.

Solvang, T., 2013. Historical Trends in Lake and River Ice Cover in Norway: Signs of a Changing Climate. Department of Geosciences, MSc. Univeristy of Oslo, Oslo, Norway.

Stéphenne, K., 2014. Start-up of world's first commercial post-combustion coal fired CCS project: contribution of shell cansolv to SaskPower boundary Dam ICCS project. Energy Proc. 63, 6106–6110.

Sørensen, L., et al., 2015. Photodegradation in natural waters of nitrosamines and nitramines derived from CO2 capture plant operation. Int. J. Greenh. Gas Control 32, 106–114.

Tan, W., et al., 2021. Experimental and theoretical study of the OH-initiated degradation of piperazine under simulated atmospheric conditions. J. Phys. Chem. 125, 411–422.

Vormoor, K., et al., 2015. Climate change impacts on the seasonality and generation processes of floods – projections and uncertainties for catchments with mixed snowmelt/rainfall regimes. Hydrol. Earth Syst. Sci. 19, 913–931.

Walse, S.S., Mitch, W.A., 2008. Nitrosamine carcinogens also swim in chlorinated pools. Environ. Sci. Technol. 42, 1032–1037.

Williams, D.J., et al., 2003. Seasonality in contaminant concentrations in the niagara river and lakes erie and ontario. J. Great Lake. Res. 29, 594–607.

Yu, K., et al., 2017. Nitrosamines and nitramines in amine-based carbon dioxide capture systems: fundamentals, engineering implications, and knowledge gaps. Environ. Sci. Technol. 51, 11522–11536.

Zhu, L., et al., 2013. Real-time monitoring of emissions from monoethanolamine-based industrial scale carbon capture facilities. Environ. Sci. Technol. 47, 14306–14314.